Scientific Research Publishing

Journal of Applied Mathematics and Physics, 2023, 11, 2361-2372
https://www.scirp.org/journal/jamp
ISSN Online: 2327-4379
ISSN Print: 2327-4352

Heat Characteristics and Viscous Flow in a Moving Isothermal Cylindrical Duct with Nanoparticles

Emmanuel O. Sangotayo[1*], Kasali A. Adedeji[2], Joel Ovo Ogidiga[1]

[1]Department of Mechanical Engineering, Ladoke Akintola University of Technology, Ogbomoso, Nigeria
[2]Department of Mechanical Engineering, Lagos State University, Epe, Lagos State, Nigeria
Email: *eosangotayo@lautech.edu.ng

How to cite this paper: Sangotayo, E.O., Adedeji, K.A. and Ogidiga, J.O. (2023) Heat Characteristics and Viscous Flow in a Moving Isothermal Cylindrical Duct with Nanoparticles. *Journal of Applied Mathematics and Physics*, **11**, 2361-2372.
https://doi.org/10.4236/jamp.2023.118151

Received: August 23, 2022
Accepted: August 21, 2023
Published: August 24, 2023

Abstract

Extrusion, melt spinning, glass fiber production, food processing, and mechanical molding rely on heat transmission. Isothermal techniques have been employed in highly structured equipment and living cell temperature regulators. The flow and heat properties of CuO nanofluids flowing through a moving cylindrical isothermal conduit were examined, in the presence of nanoparticles and viscous dissipation. Two-dimensional flows of an incompressible Newtonian fluid via a cylindrical conduit with uniform surface velocity and temperature were utilized. The flow's partial differential equations were transformed to a non-dimensional form and numerically solved using a finite difference scheme built in the C++ program. The effect of nanoparticle size (0.0 to 0.6) and viscous dissipation (0, 20, 40) on heat behavior and fluid movement are examined and profiles are used to present the numerical findings. The findings revealed that decreasing the variable nanoparticle parameter increased fluid velocity, stream function, and circulation while decreasing fluid temperature. The temperature of the fluid rises in direct proportion, as the viscous dissipation factor improves. This study improves understanding of the viscous flow and heat behavior of boundary layer problems when a nanofluid is used as the heat transfer working fluid in various engineering isothermal processes such as boiling and condensation.

Keywords

Cylindrical Duct, Finite-Difference, Isothermal, Temperature-Dependent, Viscous-Dissipation

1. Introduction

Nanofluids are colloidal suspensions generated by dispersing particles on the nanoscale scale in common base fluids. Thus, a stable, highly conducting suspension with enhanced transient thermal interactions is produced. In light of the vast potential for nanotechnology applications, nanofluids have been explored for a long time to enhance heat transfer fluids. Mixtures of sub-micron and nanometer-sized solid particles compose nanofluids. Due to the immense diversity and complexity of nanofluid systems, no consensus has emerged about the list of benefits that nanofluids may offer in thermal management applications. Several scholars have investigated the thermophysical features of nanofluids, including heat conductivity and viscosity [1] [2]. Eastman *et al.* [3] originated the notion of nanofluids by proposing that it is feasible to circumvent these century-old technological limitations by using the unique properties of nanoparticles.

Moreover, the original application area was automotive radiator systems, however, new sectors have emerged, including flame retardants [4] [5], thermal power energy [6] [7], aviation fuels [8], viscoelastic materials processing [9], tribology [10], low thermal systems, advertising heat exchangers [11], solar energy, coating security systems, mild robotics, heat technology, and ecological processes (remediation) [12]. In addition, nanoparticles of metals or metallic oxides, such as copper oxide, alumina, and titania, can flow in fluids without sinking. Hence, these nanofluids address a range of difficulties related to conventional fluid flow, such as abrasion, blockage, and higher loss, and are envisaged as another fluid for use in heat transfer technologies of the 20th century [13].

Sangotayo and Peter [14] studied the effect of the thermal characteristics of water-based nanofluids including Al_2O_3, TiO_2 and CuO on the thermal competence of the Parabolic Trough Solar Collector. When TiO_2, CuO, and Al_2O_3 are used, the heat transfer coefficient increases by 20%, 21%, and 14%, respectively, but thermal yields decrease by 9%, 56%, and 33%, while density increases by 28%, thermal conductivity increases by 23%, and specific heat capacity decreases by 30%. This demonstrates that the nanoparticles alter the thermal properties of the suspension, hence changing its applicability. Bianco *et al.* [15] investigated the hydrodynamic and thermal parameters of water-Al_2O_3 nanofluids moving inside a uniformly heated channel. The findings demonstrated that the addition of nanoparticles significantly increased the heat transfer capability of the base liquid.

Sangotayo and Hunge investigated the effect of nanoparticle volume fraction on thermophysical characteristics and convective heat transmission in a CuO nanofluid-filled square cavity. It was revealed that nanoparticle size significantly impacts how heat is carried [16]. However there have been fewer studies on the impact of nanoparticle size on the viscous flow and thermal properties of nanofluids, despite numerous researchers have developed models for estimating the particle size of nanofluids. This study investigates the impact of nanoparticle size on the viscous flow and thermal attributes of CuO, a nanofluid based on water, in a cylindrical tube.

2. Materials and Methods

The current research uses computational methods to examine the heat transfer characteristics and viscous flow trend of CuO water-based nanofluids employed as coolants in a cylindrical channel.

2.1. The Mathematical and Physical Representation

The two-dimensional steady laminar boundary layer flow of an incompressible Newtonian fluid with temperature-dependent viscosity on the surface of the cylinder is illustrated in Figure 1. T_w is the constant surface temperature, while T_∞ is the free stream temperature (where $T_w > T_\infty$). The surface is fixed with velocity U_w in the same direction as the fluid with velocity U_∞ in the free stream zone, where $U_\infty > U_w$. Figure 1 depicts the z-axis parallel to the surface and the r-axis perpendicular to it.

The flow regulating equations are made up of mass and momentum conservation equations at each point along the continuum, [17].

These formulas define a two-dimensional cylindrical domain, Equations (1), [2].

Continuity equation:

$$\frac{\partial u}{\partial z}+\frac{\partial v}{\partial r}=0 \tag{1}$$

Equations (2) and (3) are Navier-Stokes models in the r- and z-coordinates.

$$\begin{aligned}&\rho\left(\frac{\partial v_r}{\partial t}+v_r\frac{\partial v_r}{\partial r}+\frac{v_\theta}{r}\frac{\partial v_r}{\partial \theta}+v_z\frac{\partial v_r}{\partial z}-\frac{v_\theta^2}{r}\right)\\&=-\frac{\partial p}{\partial r}+\mu\left[\frac{\partial}{\partial r}\left(\frac{1}{r}\frac{\partial}{\partial r}(rv_r)\right)+\frac{1}{r^2}\frac{\partial^2 v_r}{\partial \theta^2}+\frac{\partial^2 v_r}{\partial z^2}-\frac{2}{r}\frac{\partial v_\theta}{\partial \theta}\right]+\rho g_r\end{aligned} \tag{2}$$

$$\begin{aligned}&\rho\left(\frac{\partial v_z}{\partial t}+v_r\frac{\partial v_z}{\partial r}+\frac{v_\theta}{r}\frac{\partial v_z}{\partial \theta}+v_z\frac{\partial v_z}{\partial z}\right)\\&=-\frac{\partial p}{\partial z}+\mu\left[\frac{1}{r}\frac{\partial}{\partial r}\left(r\frac{\partial v_z}{\partial r}\right)+\frac{1}{r^2}\frac{\partial^2 v_z}{\partial \theta^2}+\frac{\partial^2 v_z}{\partial z^2}\right]+\rho g_z\end{aligned} \tag{3}$$

The formula for thermal energy exchange using Equation (4)

$$\rho c_p\left(u\frac{\partial T}{\partial r}+v\frac{\partial T}{\partial z}\right)=k\left(\frac{\partial T}{\partial r^2}+\frac{\partial T}{\partial z^2}\right)+\mu\varphi \tag{4}$$

where ϕ is the function of viscous heat transfer as expressed in Equation (5)

$$\varphi=2\left(\left(\frac{\partial u}{\partial z}\right)^2+\left(\frac{\partial v}{\partial r}\right)^2\right)+\left(\frac{\partial v}{\partial z}+\frac{\partial u}{\partial r}\right)^2 \tag{5}$$

where the nanofluid heat capacity is $(C_p)_{nf}$, density is ρ_{nf}, thermal expansion coefficient is β_{nf}, and thermal diffusivity is α_{nf} as expressed in Equations (6)-(11) [17] [18]

$$\rho_{nf}=(1-\varphi)\rho_f+\varphi\rho_s \tag{6}$$

$$(\rho C_p)_{nf}=(1-\varphi)(\rho C_p)_f+\varphi(\rho C_p)_s \tag{7}$$

$$(\rho\beta)_{nf}=(1-\varphi)(\rho\beta)_f+\varphi(\rho\beta)_s \tag{8}$$

$$\alpha_{nf}=\frac{k_{nf}}{(\rho C_p)_{nf}} \tag{9}$$

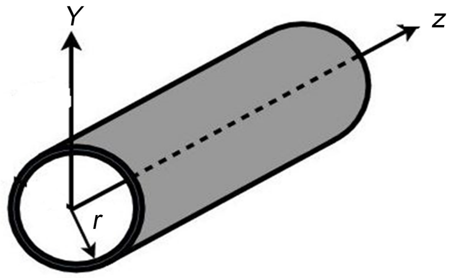

Figure 1. A schematic representation illustrating the physical state and boundary conditions of an isothermal cylinder wall.

The dynamic viscosity of the nanofluid is calculated using the Brinkman theory in Equation (10), [17] [18]

$$\mu_{eff} = \frac{\mu_f}{(1-\varphi)^{2.5}} \tag{10}$$

The effective thermal conductivity (k_{nf}) of the nanofluid-containing nanospheres is computed using Equation (11) [17].

$$\frac{k_{nf}}{k_f} = \frac{k_s + 2k_f - 2\varphi(k_f - k_s)}{k_f + 2K_s + \varphi(k_f - k_s)} \tag{11}$$

2.2. Methods of Analysis and Strategies of Solution

The Navier-Stokes models are a form of partial differential equation that can be hyperbolic elliptic, or parabolic, according to the application. These formulae can be resolved using either the vorticity-stream variable method or the primitive-variable approach. Using the vorticity-stream feature approach, formulas (2) and (3) are simplified to vorticity transport formulas by expelling the pressure gradient concepts between the two, utilizing the continuity model (1) and the expression for the scalar worth of the vorticity, in the two-dimensional polar coordinate scheme described by the vorticity-stream feature, Equation (12)

$$\omega = \frac{\partial v}{\partial r} - \frac{\partial u}{\partial z}. \tag{12}$$

The resultant statement, equation, is the dimensional vorticity transfer (13)

$$u\frac{\partial \omega}{\partial r} + v\frac{\partial \omega}{\partial z} = -\beta g\frac{\partial T}{\partial r} + \upsilon\left(\frac{\partial^2 \omega}{\partial r^2} + \frac{\partial^2 \omega}{\partial z^2}\right) \tag{13}$$

The derivatives of the stream function are used to describe the velocity field in two-dimensional cylindrical coordinate, Equation (14)

$$u = \frac{\partial \psi}{\partial z}, \quad v = -\frac{\partial \psi}{\partial r} \tag{14}$$

When substituted in Equation (12), it provides the Poisson formula, Equation (15)

$$\omega = -\left(\frac{\partial^2 \psi}{\partial r^2} + \frac{\partial^2 \psi}{\partial z^2}\right) \tag{15}$$

The resulting transport formula, energy model, and needed operating conditions were all converted to a non-dimensional formulation for various physical situations utilizing such as U_W, $\psi_W L$, L, ω_W/L and $(T_w - T_\infty)$, respectively for velocity, stream function, length, vorticity, and temperature, [19].

$$R = \frac{r}{L},\quad Z = \frac{z}{L},\quad U = \frac{u}{U_w},\quad V = \frac{v}{U_w},$$

$$\theta = \frac{T - T_\infty}{T_w - T_\infty},\quad \Psi = \frac{\psi}{U_w L},\quad \Omega = \frac{\omega}{U_w/L},$$

The following are the normalized formulas for the R- and Z-velocity elements, the stream component, vortex shedding, and energy transit as expressed in Equation (16)-(19):

$$u = \frac{\partial \varphi}{\partial Z},\quad V = -\frac{\partial \varphi}{\partial R} \tag{16}$$

$$\omega = -\frac{\partial^2 \varphi}{\partial Z^2} - \frac{\partial^2 \varphi}{\partial R^2} \tag{17}$$

$$u\frac{\partial \omega}{\partial Z} - V\frac{\partial \omega}{\partial R} = BRaPr\frac{\partial \theta}{\partial Z} + A\left(\frac{\partial^2 \omega}{\partial Z^2} + \frac{\partial^2 \omega}{\partial R^2}\right) \tag{18}$$

where $A = \frac{\mu_{nf}}{\rho_{nf}\alpha_{nf}}$, $B = \frac{(\rho\beta)_{nf}}{\rho_{nf}\beta_f}$,

$$Pr = \frac{V_f}{\alpha_f},\quad Pr_{nf} = \frac{V_{nf}}{\alpha_{nf}}$$

$$u\frac{\partial \theta}{\partial Z} + V\frac{\partial \theta}{\partial R} = \frac{\alpha_{nf}}{\alpha_f}\left(\frac{\partial^2 \theta}{\partial Z^2} + \frac{\partial^2 \theta}{\partial R^2}\right) \tag{19}$$

where μ represents dynamic viscosity, k represents thermal conductivity, *Re* represents Reynolds number, *Gr* represents Grashof number and *Cp* represents specific heat capacity,

The non-dimensional boundary situations are as follows:

$$\Psi \neq 0; V = 0; \Omega \neq 0; \theta = U = 1 \text{ at } Z = 1;\ 0 \le R \le 1;$$

$$\Psi = V = U = \theta = 0; \Omega \neq 0; \text{ at } Z = 0; 0 \le R \le 1;$$

$$\theta = \Psi = V = U = 0; \Omega \neq 0 \text{ at } R = 0; 0 \le Z \le 1;$$

$$\Psi = \frac{\partial V}{\partial R} = \frac{\partial U}{\partial R} = \frac{\partial \theta}{\partial R} = 0; \Omega \neq 0 \text{ at } R = 1; 0 \le Z \le 1.$$

In nonlinear Equations (18) and (19) for vorticity and energy transport, the finite difference technique is one of the most successful methods for problem-solving (16)-(19). The relaxation approach was used to evaluate the concurrent system of equations. According to formula (20), the temperature gradient induced by heat transmission between a fluid and a wall is proportional to the neighbouring Nusselt number.

$$Nu_x = \frac{h_x r}{k} = -\left(\frac{\partial \theta}{\partial Z}\right)_{Z=1} \tag{20}$$

The typical Nusselt quantity is obtained by integrating the enclosed Nusselt number over the distance of the heated surface, as shown in Equation (21)

$$N\overline{u} = \frac{\dot{Q}_{conv}}{\dot{Q}_{cond}} = -\int_0^1 \frac{\partial \theta}{\partial Z}\bigg|_{Z=0 \text{ or } 1} \mathrm{d}R \tag{21}$$

The stable flow requirement was achieved by setting for agreement in the vortex and temperature fields, as indicated in Equation (22)

$$\frac{\sum_{i=2}^{N}\sum_{j=2}^{M}\left|\phi_{ij}^{n+1} - \phi_{ij}^{n}\right|}{\sum_{i=2}^{N}\sum_{j=2}^{M}\left|\phi_{ij}^{n+1}\right|} < \delta \tag{22}$$

The variable ϕ denotes Ω, Ψ or θ and n is the number of iterations required for the outputs to converge. The value used varies between 10^{-3} and 10^{-8} in diverse literature [20].

3. Results and Discussions

The local Nusselt number was determined at different convergence factor values ranging from 10^{-1} to 10^{-8} to analyze the influence of the convergent standard on numerical results and **Figure 2** depicts the outcomes. It illustrates that a quantity of 10^{-4} for the convergence factor was appropriate. According to Waheed [21], grid independence tests indicated that a 41 by 41 grid design is sufficient for exceptional numerical solution, field precision, and high accuracy.

The non-dimensional temperature trend for different Eckert numbers (0, 20, and 40). is shown in **Figure 3**. As the Eckert number increases, the temperature distribution along z increases significantly from 0.0 to 0.1, mid-plane, $r = 0.5$, enhancing the temperature gradient. It implies that viscous action enhances thermal characteristics.

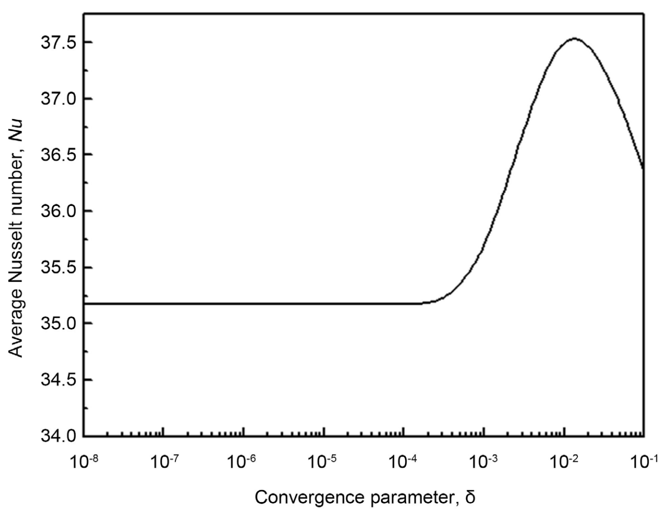

Figure 2. A graph of the mean Nusselt number, *Nu*, versus convergence variable, δ.

The effect of altering the Eckert number between 0 and 50 on the Nusselt number is visualized in **Figure 4**. The Nusselt values grow in lockstep with the viscous values, confirming the observations of Sangotayo and Hunge [16]. It means that convective heat transfer is rapidly increasing while conduction heat transfer is decreasing.

Figure 5 displays the influence of nanoparticle size on CuO nanofluid temperature at the mid-plane, $r = 0.5$, along the Z-axis. The temperature distribution along z increases from 0.0 to 0.1 as particle size increases from 0 to 0.6. That is, the particle size effect increases the temperature gradient. The findings corresponded with those of Umavathi and Bég [13].

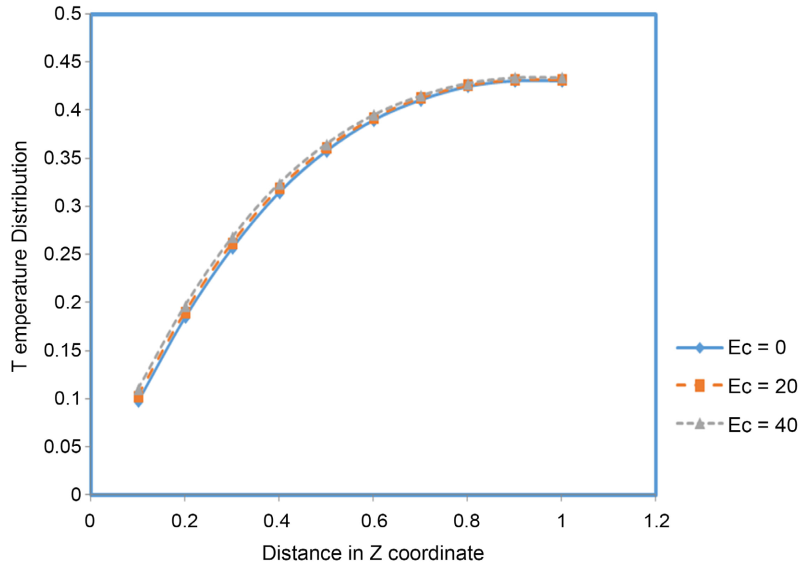

Figure 3. The normalized temperature curve at different Eckert numbers along the Z direction.

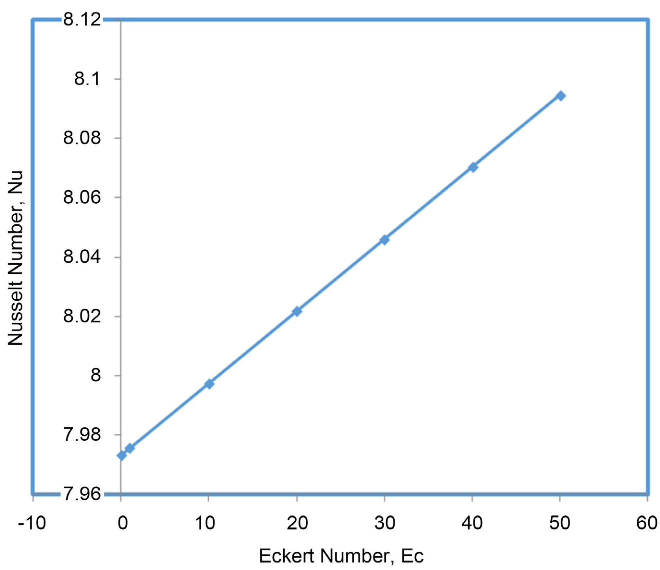

Figure 4. The influence of altering the Eckert number on the Nusselt number.

The influence of nanoparticle sizes on the longitudinal velocity of CuO nanofluid on a plane with $r = 0.5$ along the z axis is shown in Figure 6. The longitudinal velocity distribution decreases as the particle size increases from 0 to 0.6. It implies that nanofluids with smaller particle sizes improve flow patterns.

The influence of nanoparticle size on the vorticity of a nanofluid is depicted in Figure 7. The particle size grows as the vorticity of the nanofluid drops. The vorticity distribution decreases as the particle size increases from 0 to 0.6. This

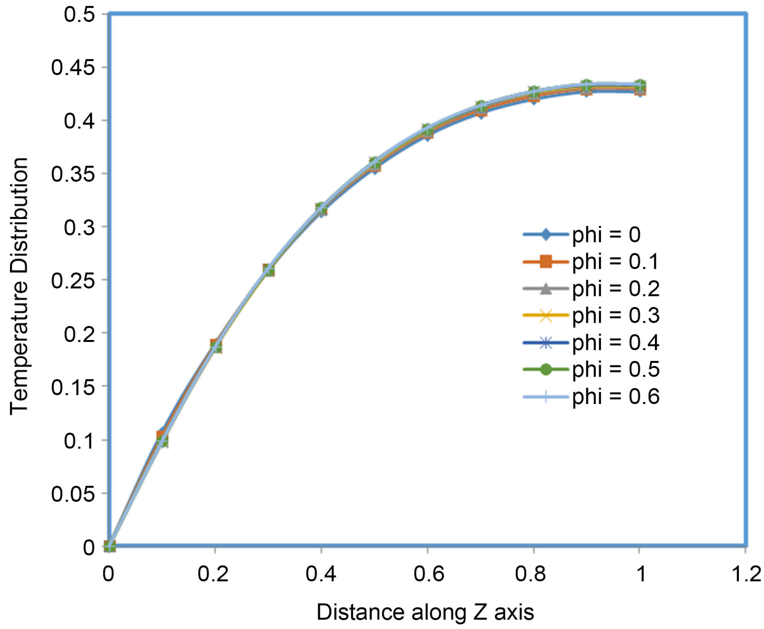

Figure 5. Temperature curve of several nanoparticles along the Z-axis at the plane's midpoint, $r = 0.5$.

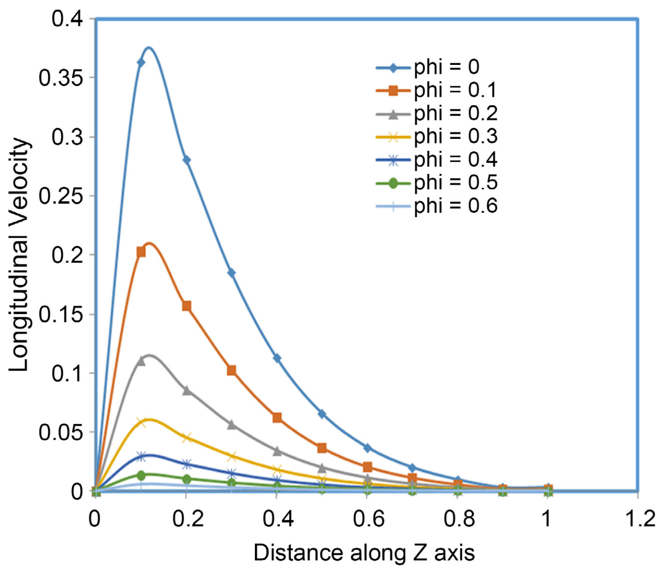

Figure 6. Longitudinal Velocity trajectories of several nanoparticles along the Z-axis at the centerline.

suggests that nanofluids with smaller particle sizes improve flow circulation and rotation patterns. Both circulation and vorticity are indicators of fluid rotation. A circulation is a macroscopic unit of rotation for a finite-area fluid. Vorticity is a microscopic characteristic that describes how any point in a fluid rotates. Figure 8 shows the Stream function for nanofluid plotted against the concentration of nanoparticles. It implies that as particle size enlarges, the stream function of the nanofluid diminishes, resulting in a drop in the volume flow rate across the tube of the nanofluids. The results were consistent with those of Uddin *et al.* [22].

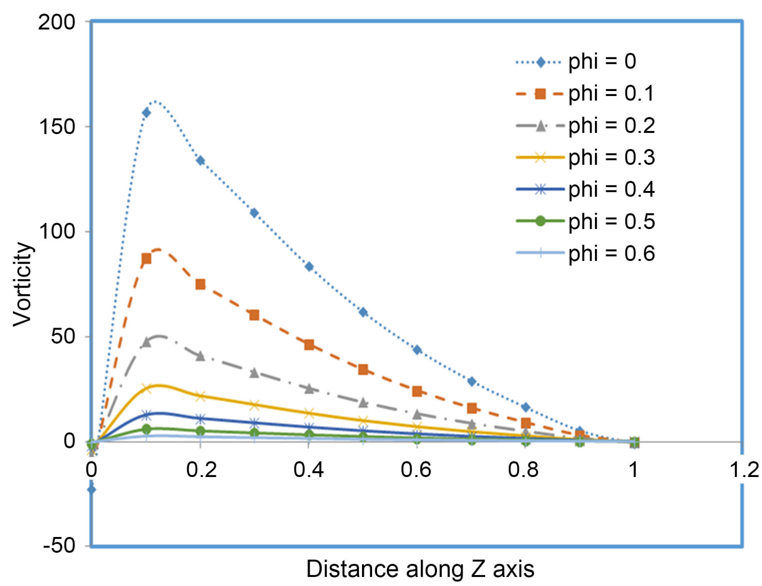

Figure 7. Vorticity patterns for various nanoparticles along the Z-axis at the plane's midpoint, $r = 0.5$.

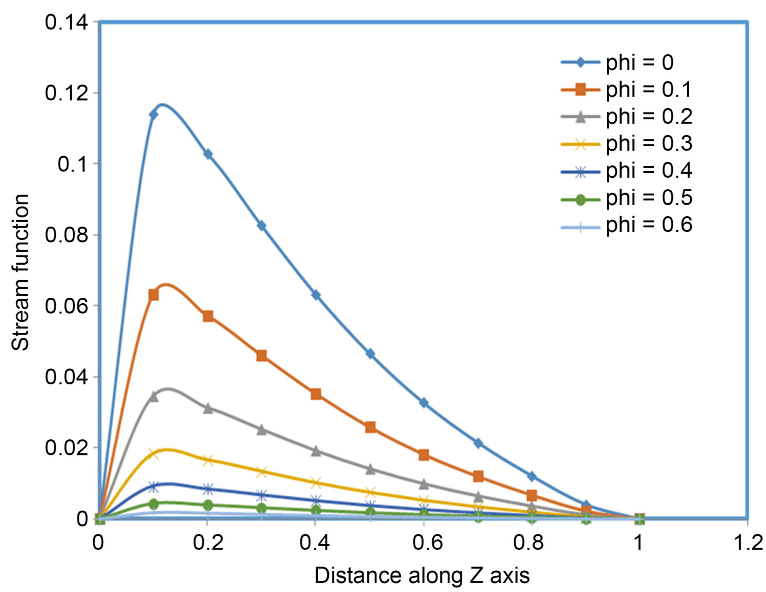

Figure 8. Stream function curves of various nanoparticles along the Z-axis at the centerline, $r = 0.5$.

4. Conclusion

The heat transfer fluids influence the size and cost of heat exchangers. Numerical modeling was used to investigate the impact of nanoparticles on viscous flow and heat transfer in a moving isothermal cylindrical duct. The findings show that the nanofluids' temperature rises with the nanoparticles' size. The stream function, longitudinal velocity, rotation, and circulation all decline when the concentration of nanoparticles increase. This research shows that incorporated nanoparticles change a suspension's thermal characteristics, affecting its application. Addition of nanoparticles and using a nanofluid as a heat transfer working fluid in engineering isothermal phenomena as boiling and condensation improves knowledge of viscous flow and heat response of boundary layer issues.

Conflicts of Interest

The authors declare no conflicts of interest regarding the publication of this paper.

References

[1] Wen, D.S., Lin, G.P., Vafaei, S. and Zhang, K. (2009) Review of Nanofluids for Heat Transfer Applications. *Particuology*, **7**, 141-150. https://doi.org/10.1016/j.partic.2009.01.007

[2] Wang, X.Q. and Mujumdar, A.S. (2007) Heat Transfer Characteristics of Nanofluids: A Review. *International Journal of Thermal Sciences*, **46**, 1-19. https://doi.org/10.1016/j.ijthermalsci.2006.06.010

[3] Eastman, J.A., Choi, S.U.S., Li, S., Yu, W. and Thompson, L.J. (2001) Anomalously Increased Effective Thermal Conductivities of Ethylene Glycol-Based Nanofluids Containing Copper Nanoparticles. *Applied Physics Letters*, **78**, 718-720. https://doi.org/10.1063/1.1341218

[4] Tentu, N., Rao, I.H. and Bon, H.K. (2020) Enhanced Thermal Properties of Silica Nanoparticles and Chitosan Bio-Based Intumescent Flame-Retardant Polyurethane Coatings. *Materials Today*: *Proceedings*, **27**, 369-375. https://doi.org/10.1016/j.matpr.2019.11.153

[5] Umavathi, J.C., Bég, O.A., Gorla, R.S.R. and Vasu, B. (2020) Perturbation and MAPLE Quadrature Computation of Thermosolutal Dissipative Reactive Convective Flow in a Geothermal Duct with Robin Boundary Conditions. *TFRE* 2020: *International Conference on Recent Trends in Developments of Thermo-Fluids and Renewable Energy*, Yupia, 24-26 June 2020, 3-21. https://doi.org/10.1007/978-981-16-3497-0_1

[6] Xiu, T.F. (2016) Al-Nanoparticle-Containing Nanofluid Fuel: Synthesis, Stability, Properties, and Propulsion Performance. *Industrial & Engineering Chemistry Research*, **55**, 2738-2745. https://doi.org/10.1021/acs.iecr.6b00043

[7] Umavathi, J.C. and Bég, O.A. (2020) Modelling the Onset of Thermosolutal Convective Instability in a Non-Newtonian Nanofluid-Saturated Porous Medium Layer. *Chinese Journal of Physics*, **68**, 147-167. https://doi.org/10.1016/j.cjph.2020.09.014

[8] Zhang, Y. (2016) Experimental Study on the Effect of Nanoparticle Concentration on the Lubricating Property of Nanofluids for MQL Grinding of Ni-Based Alloy. *Journal of Materials Processing Technology*, **232**, 100-115. https://doi.org/10.1016/j.jmatprotec.2016.01.031

[9] Umavathi, J.C., Ojjela, O. and Vajravelu, K. (2017) Numerical Analysis of Natural Convective Flow and Heat Transfer of Nanofluids in a Vertical Rectangular Duct Using Darcy-Forchheimer-Brinkman Model. *International Journal of Thermal Sciences*, **111**, 511-524. https://doi.org/10.1016/j.ijthermalsci.2016.10.002

[10] Tripathi, J., Vasu, B. and Bég, O.A. (2021) Computational Simulations of Hybrid Mediated Nano-Hemodynamics (Ag-Au/Blood) through an Irregular Symmetric Stenosis. *Computers in Biology and Medicine*, **130**, Article ID: 104213. https://doi.org/10.1016/j.compbiomed.2021.104213

[11] Hu, Z.L., *et al*. (2016) Nanoparticle-Assisted Water-Flooding in Berea Sandstones. *Energy Fuels*, **30**, 2791-2804. https://doi.org/10.1021/acs.energyfuels.6b00051

[12] Dickinson, E. (2012) Use of Nanoparticles and Microparticles in the Formation and Stabilization of Food Emulsions. *Trends in Food Science & Technology*, **24**, 4-12. https://doi.org/10.1016/j.tifs.2011.09.006

[13] Umavathi, J.C. and Bég, O.A. (2021) Augmentation of Heat Transfer via Nanofluids in Duct Flows Using Fourier-Type Conditions: Theoretical and Numerical Study. *Proceedings of the Institution of Mechanical Engineers*, *Part E*: *Journal of Process Mechanical Engineering*, **236**, 926-941. https://doi.org/10.1177/09544089211052025

[14] Sangotayo, E.O. and Peter, B.A. (2020) Comparative Assessment of the Effect of Thermo-Physical Properties on the Performance of Parabolic Trough Solar Collector. *Journal of Applied Sciences*, *Information*, *and Computing*, **1**, 9-19. https://jasic.kiu.ac.ug https://doi.org/10.59568/JASIC-2020-1-1-02

[15] Bianco, V., Chiacchio, F., Manca, O. and Nardini, S. (2009) Numerical Investigation of Nanofluids Forced Convection in Circular Tubes. *Applied Thermal Engineering*, **29**, 3632-3642. https://doi.org/10.1016/j.applthermaleng.2009.06.019

[16] Sangotayo, E.O. and Hunge, O.N. (2019) Numerical Analysis of Nanoparticle Concentration Effect on Thermo-Physical Properties of Nanofluid in a Square Cavity. *Proceeding of WRFASE International Conference*, Abu Dhabi, 28 November 2019, 5-10.

[17] Ozisik, M.N. (1985) Heat Transfer, a Basic Approach. International Textbook Company, Sheraton.

[18] Kalbasi, M. and Saeedi, A. (2012) Numerical Investigation into the Convective Heat Transfer of CuO Nanofluids Flowing through a Straight Tube with Uniform Heat Flux. *Indian Journal of Science and Technology*, **5**, 2455-2458. https://doi.org/10.17485/ijst/2012/v5i3.39

[19] Kalteh, M., Abbassi, A., Saffar-Avval, M. and Harting, J. (2011) Eulerian Two-Phase Numerical Simulation of Nanofluid Laminar Forced Convection in a Microchannel. *International Journal of Heat and Fluid Flow*, **32**, 107-116. https://doi.org/10.1016/j.ijheatfluidflow.2010.08.001

[20] Chung, T.J. (2002) Computational Fluid Dynamics. Cambridge University Press, Cambridge.

[21] Waheed, M.A. (2009) Mixed Convective Heat Transfer in Rectangular Enclosures Driven by a Continuously Moving Horizontal Plate. *International Journal of Heat and Mass Transfer*, **52**, 5055-5063. https://doi.org/10.1016/j.ijheatmasstransfer.2009.05.011

[22] Uddin, M., Alim, M. and Rahman, M. (2019) MHD Effects on Mixed Convective Nanofluid Flow with Viscous Dissipation in Surrounding Porous Medium. *Journal of Applied Mathematics and Physics*, **7**, 968-982. https://doi.org/10.4236/jamp.2019.74065

Nomenclature

Nu	Nusselt number
Re	Reynolds number
Gr	Grasshof number
Pr	Prandtl number
Cp	Specific heat
h	Heat transfer coefficient
K	Thermal conductivity
m	Mass flow rate
Greek symbols	
μ	viscosity
ρ	Density
φ	Volume fraction
Subscripts	
Bf	Base Fluid
nf	Nanofluid
p	Particle
f	Fluid

Symbols	**Definition**	**Unit**
C_p	Heat capacity	J/kg·K
Cp_f	Heat capacity of fluid	J/kg·K
Cp_{nf}	Heat capacity of nanofluid	J/kg·K
Cp_p	Heat capacity of nanoparticle	J/kg·K
K_f	Thermal conductivity of fluid	W/m·K
K_{nf}	Thermal conductivity of nanofluid	W/m·K
K_p	Thermal conductivity of nanoparticle	W/m·K
m	Mass flow rate	kg/hr
Qu	Useful energy	W

Greek Symbols

Symbols	**Definition**	**Unit**
φ	nanoparticle size	
ρ_{nf}	Density of nanofluid	kg/m^3
ρ_f	Density of fluid	kg/m^3
ρ_p	Density of nanoparticle	kg/m^3
μ_{nf}	Viscosity of nanofluid	m^2/s
μ_f	Viscosity of fluid	m^2/s